CURE PROCESS MONITORING OF CURVED COMPOSITE WITH INTERLAMINAR TOUGHENED LAYERS

Keiichiro Sawaguchi, Kazunori Takagaki, Shu Minakuchi and Nobuo Takeda

The University of Tokyo, Graduate School of Frontier Science, 5-1-5, Kashiwanoha, Kashiwashi, Chiba 277-8561, Japan, sawaguchi@smart.k.u-tokyo.ac.jp.

Keywords: Curved composite, Interlaminar toughened layers, Optical fiber sensors, Cure induced strain/deformation, In-situ monitoring

ABSTRACT

L-shaped composites are fundamental parts for complex-shaped structures. It is known that chemical-cure and thermal shrinkage decreases the enclosed angle (i.e., spring-in) due to its orthotropic nature, resulting in cost-intensive manual shimming during assembly. Although a lot of studies have addressed this issue, the mechanisms of spring-in deformation are not still clear. Meanwhile, recent aerospace grade Carbon fiber reinforced plastics (CFRPs) utilize interlaminar toughened layers to enhance the interlaminar fracture toughness for impact resistance. Even though interlaminar layers would significantly affect residual deformations, their effects have not been evaluated. Therefore, this study investigated the effect of interlaminar layers on the internal strain states during curing and the spring-in deformation after curing. Fiber Bragg grating (FBG) sensors were embedded into the through-thickness diagonal directions to measure the out-of-plane normal and shear strain development. The sensors captured different strain development between the CFRP parts with and without the interlaminar toughened layers, indicating that the interlaminar layer affects the internal strain development. In the part with interlaminar layers, the shear strain arose in the early stage of cure reaction and relaxed in the latter stage likely due to the stress relaxation within the interlaminar layers. As a result of experiments with different holding time, it was confirmed that the spring-in angle decreased as the curing time became longer. This result indicates that the effect of the interlaminar resin layer on the residual deformation should be considered to determine optimized cure process.

1. INTRODUCTION

CFRPs have been applied to aircraft structures due to its weight reduction advantage and environmental stability. L-shaped composites are fundamental parts for these complex-shaped structures and residual deformation (i.e., spring-in) occurs after curing due to its orthotropic nature (Fig. 1). When the spring-in deformation is corrected during assembly, significantly high out-of-plane stress is generated at the corner part, which leads to strength reduction. For this reason, optimization of tools and curing cycles has been carried out based on trial and error. However, the cost for trial manufacturing is very high, so understanding this phenomena and predicting the residual deformation based on its mechanism are quite important to determine an appropriate process in a reasonable manner with minimal trial and error.

So far, various research on spring-in has been carried out. Radford [1] predicted spring-in angles based on geometric calculations by the following equation.

$$\Delta\theta = \theta\left(\frac{\Delta\varepsilon_I - \Delta\varepsilon_T}{1+\Delta\varepsilon_T}\right) = \theta\left(\frac{(\alpha_I - \alpha_T)\Delta T}{1+\alpha_T \Delta \mathrm{T}}\right) + \theta\left(\frac{\phi_I - \phi_T}{1+\phi_T}\right) \quad (1)$$

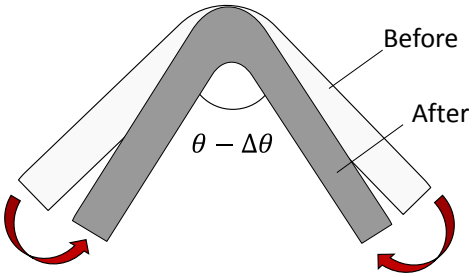

Figure. 1: Spring-in deformation.

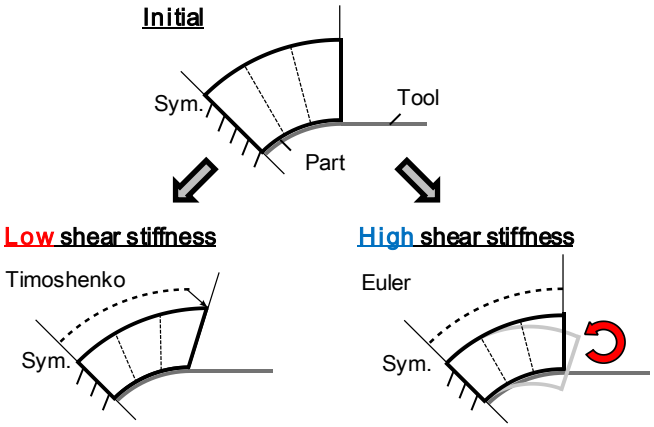

Fig. 2: Schematic of shear-lag analysis

where θ is the angle of the corner part, ε is the strain, α is the thermal expansion coefficient, ΔT is the temperature change, ϕ is the cure expansion strain, and the subscripts I and T indicate the in-plane and out-of-plane directions. However, this formula cannot explain the effect of thickness as measured in most experiments. Therefore, Wisnom et al. [2] formulated the assumption that shear deformation in the thickness direction occurs when the resin modulus is low in the first half of chemical cure reaction, according to the Shear-lag theory for C-shaped part (Fig. 2). They considered that through-thickness normal strain induces shear deformation to maintain the same arc length if the shear modulus is negligible, which generates no residual deformation. In contrast, if shear stiffness is high, through-thickness shrinkage is accommodated by in-plane stress (i.e., bending deformation) and no shear deformation is generated, resulting in spring-in after removal from the tool, which is geometrically calculated in Eq. (1). In practice, a curing composite takes a middle position between these two extreme cases, leading to residual deformation depending on the ratio of shear and bending deformation. Theoretical analysis successfully predicted the effect of thickness as obtained in the corresponding experiment. Takagaki et al. [3] expanded this model to practically relevant L-shaped parts and clarified their behavior in detail by employing in-situ monitoring of the internal strain.

Meanwhile, recent aerospace grade CFRPs utilize interlaminar toughened layers to enhance the interlaminar fracture toughness for impact resistance (Fig. 3). Albert and Fernlund [4] measured spring-in angles using a material with interlaminar resin layers while changing stacking sequence, thickness, flange length and cure cycle. However the influence of interlaminar resin layers on the spring-in deformation has not been clarified. Although it is expected that the out-of-plane shear deformation generated during curing is influenced by the resin layers, sufficient knowledge has not been obtained at present. Therefore, this study evaluates the effect of the interlaminar resin layers on shear and bending deformation generated during curing and on the final spring-in angle.

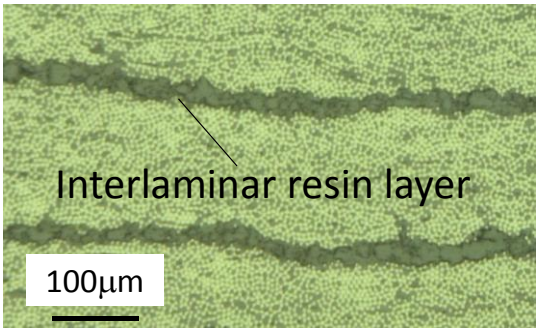

Fig. 3: Interlaminar resin layer.

2 Internal Strain Measurement Using Optical Fiber Sensors

2.1 FBG sensor

In this study, internal strain was measured using fiber Bragg grating (FBG) sensors which are one type of optical fiber sensors (Fig. 4). FBG has a sensing part in the core in which the refractive index is periodically changed. Narrow band light is reflected when broadband light is launched into the FBG and the central wavelength of the reflected light called a Bragg wavelength shifts by temperature and strain changes in the FBG sensor.

$$\Delta\lambda = C_\varepsilon \Delta\varepsilon + C_t \Delta T \tag{2}$$

$\Delta\lambda$ is the change in the center wavelength, $\Delta\varepsilon$ is the strain change, ΔT is the temperature change, and C_ε and C_t are the constants. By compensating the temperature contribution using a thermocouple, it is possible to calculate the strain from the change in the Bragg wavelength. In this study, the FBG sensor is embedded into the $\pm 45°$ through-thickness directions. The strain captured by these two sensors is expressed as follows,

$$\begin{aligned} \varepsilon_{+45} &= \frac{1}{2}(\varepsilon_l + \varepsilon_t + \gamma_{tl}) \\ \varepsilon_{-45} &= \frac{1}{2}(\varepsilon_l + \varepsilon_t - \gamma_{tl}) \end{aligned} \tag{3}$$

where ε_t is the out-of-plane normal strain, ε_l is the in-plane strain and γ_{tl} is the out-of-plane shear strain. The in-plane strain ε_l is negligible compared to the other two strains because the in-plane deformation is constrained by the carbon fibers. So the out-of-plane normal and shear strain can be calculated by summation and subtraction of these two sensor responses.

2.2 Experimental method

Cure-induced strain monitoring was conducted using FBG sensors diagonally embedded into the ±45° through-thickness directions (Fig. 5). T800S/3900-2B (Toray Industries, Inc.) with interlaminar resin

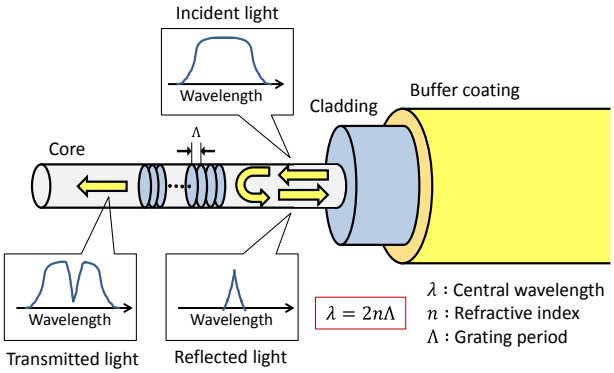

Fig. 4: Schematic of structure and measurement principle of FBG sensor

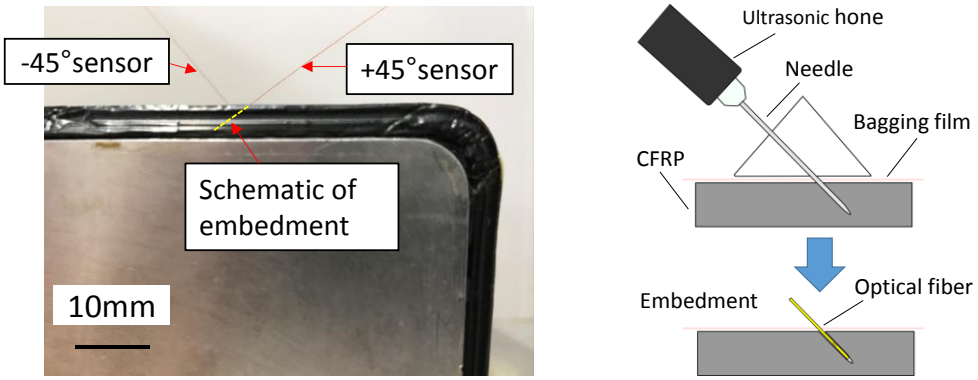

Fig. 5: Photograph of diagonal FBG sensors and FBG embedment method.

layers was used to be compared with the result of a material without interlaminar resin layers (T700/2592 (Toray Industries, Inc.)) [3]. The stacking sequence was $[90_4/0_4]_{2S}$ (90° was the longitudinal direction), the corner radius was 6.4 mm, the flange length was 60 mm, and the width was 75 mm. Prepreg sheets were first laid up on a tool made of aluminum and vacuum bagging was applied. A small hole was then introduced in the prepreg sheets and the bag film using an ultrasonic horn and a metal needle (ϕ = 0.5 mm), and finally an FBG sensor (grating length: 1 mm) was inserted (Fig. 5). The FBG sensor was cut at 2 mm from the grating and the sensing part was located at the center in the thickness direction of the laminate. The sensors were embedded at positions 30 mm away from the edge of the flange so as to eliminate the edge effect on the sensor response. The distance between the two optical fibers was 20 mm. After embedding, sealant tape was used to cover the hole in the bag film. The curing was conducted in an autoclave under 0.6 MPa pressurization with 2°C/min heating, 180°C holding for 4 hours and 2°C / min cooling.

3 Test Results and Discussion

3.1 Out-of-plane normal and shear strain

The out-of-plane normal and shear strains measured by the FBG sensors embedded in the ±45° directions are shown in Fig. 6(a). The results of the previous study (T700S/2592 without interlaminar resin layers) are also presented in Fig. 6(b) [3]. As a common phenomenon in both materials, both normal and shear strains changed similarly just after gelation and the shear strain changing rates decreased afterward. Thus, it was confirmed that the ratio of the shear deformation was large at the beginning of the chemical cure reaction, whereas shear deformation was suppressed afterward and the ratio of bending deformation increased (Fig. 2). During cooling shear strain was hardly measured, so bending deformation was dominant as the latter part of chemical cure reaction. As for the different phenomena in both materials, the material with the interlaminar resin layers had large changes in both out-of-plane normal and shear strain (Fig. 7). In addition, shear strain was relaxed during the temperature hold (Fig: 7(a)). This strain relaxation may be attributed to the stress relaxation in the interlaminar resin layers constituted by thermoplastic particles and epoxy resin as discussed in [5]. Fig: 8 shows the results of the strain development of both material types plotted against temperature. Both shear and normal strain decreased linearly during cooling in the material without interlaminar resin layers but in the material with interlaminar resin layers the change in coefficient of thermal expansion was observed around 140°C. This result indicates that the internal strain and stress change complicatedly due to the interlaminar resin layers.

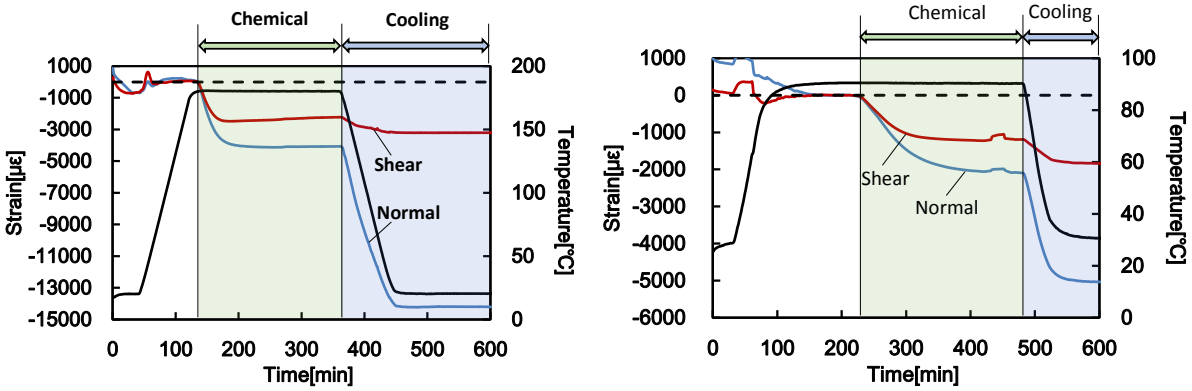

(a) (b)

Fig. 6: Cure-induced strain development:
(a)Normal and shear strain of CFRP with interlaminar resin layers.
(b)Normal and shear strain of CFRP without interlaminar resin layers [3].

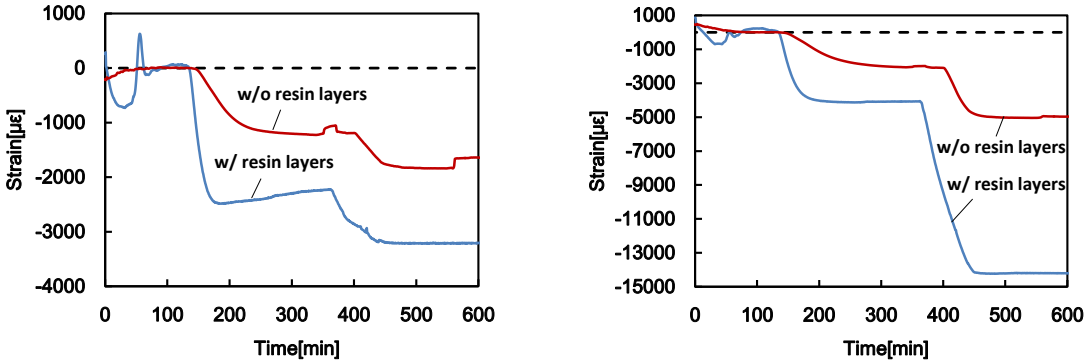

(a) (b)

Fig .7: Comparison of strain development in materials with and without interlaminar layers:
(a) Out-of-plane shear strain. (b) Out-of-plane normal strain.

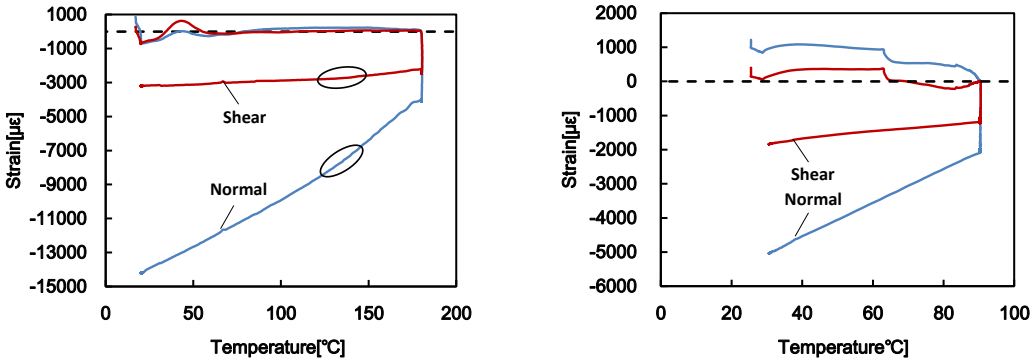

(a) (b)

Fig. 8: Cure induced strain history plotted against temperature:
(a) CFRP with interlaminar resin layers. (b) CFRP without interlaminar resin layers [3].

3.2 Spring-in angle

The strain relaxed in the latter part of the chemical cure reaction seen in Fig: 7(a) was a very small value compared to the whole cure strain, but it was expected that the relaxed stress was large because the material was vitrified and had a high stiffness at this stage. In order to investigate the effect of this stress relaxation on the final shape, L-shaped parts were cured using two cycles with different 180°C

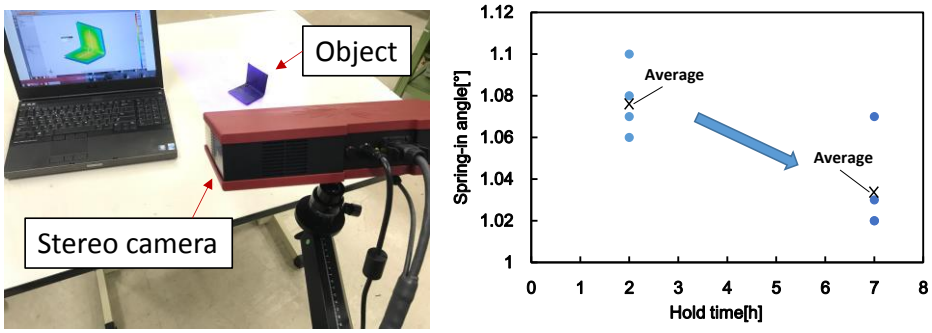

Fig. 9: 3D shape scanning using optical measurement system (ATOS) and the change in spring-in angle.

holding time; 2 hours and 7 hours. The final spring-in angle depending on the cure cycle was evaluated.

Spring-in angle was measured using an instrument ATOS (GOM mbH, Germany) (Fig. 9). Four specimens were cured using each holding time and an average of the spring-in angle was calculated. On average, the test part with the holding time of 7 hours had a spring-in angle 0.04 degree less than the test part of 2 hours. This is probably because each layer partly deformed as an independent plate due to stress relaxation in the interlaminar resin layers. As a result, the flexural rigidity of the entire L-shaped part decreased and the bending stress induced by chemical cure shrinkage was relaxed, leading to less spring-in deformation after demolding. This angle change is relatively small but cannot be neglected as aerospace-grade components must meet tight tolerances. In case that dimensional tolerance is 0.25 mm, acceptable deformation is exceeded at a position 350 mm away from the corner part. It is important to note that in this study the cure temperature holding time was intentionally changed, but temperature history actually differs within a large-scale part under a practical manufacturing process as the part and tool thickness is non-uniform and each area has different heating rate and cure temperature holding time. So it is expected that the deformation amount may differ even in actual manufacturing.

4 Conclusion

L-shaped CFRPs are important and fundamental structure parts in aerospace applications and residual deformation occurs after curing due to the influence of its orthotropic nature. Moreover recent aerospace-grade CFRPs utilize interlaminar resin layers to enhance the fracture toughness for high impact resistance, and it is necessary to consider the effect of its resin layers on spring-in deformation.

In this study, in-situ strain measurement was carried out during curing using FBG sensors embedded into the ± 45 ° out-of-plane directions, and the through-thickness normal and shear strain was obtained from the sensor responses. It was found that the shear deformation ratio was large at the beginning of chemical cure reaction but shear deformation was suppressed afterward. In addition, in the material with interlaminar resin layers, the shear strain relaxed during cure temperature hold time probably due to stress relaxation. The experiment with changing holding time confirmed that longer holding leads to smaller spring-in angle. Future work will address this mechanism by using finite element analysis.

Acknowledgments

This research was conducted by the Strategic Innovation Promotion Program (SIP) "Structural Materials" (Management Corporation: JST) of the Cabinet Office's General Science and Technology Innovation Conference.

REFERENCES

[1] Radford D.W, R.J. Diefendorf. 1993. “Shape instabilities in composites resulting from laminate anisotropy.” *J. Reinf. Plast. Compos.*, 12(1):58-75.

[2] Wisnom M.R., K.D. Potter, and N. Ersoy. 2006. ”Shear-lag analysis of the effect on thickness on

spring-in of curved composites" *J. Compos. Mater.,* 41(11): 1311-1324.
[3] Takagaki K, et al. 2017. "Evaluating cure-induced internal strain and distortion mechanism of complex-shaped CFRP" PhD Thesis, The University of Tokyo, Japan.
[4] Albert C., and G. Ferlund. 2002."Spring-in and warpage of angled composite laminates." *Compos. Sci. Technol.,* 62(14):1895-1912.
[5] Niwa S, et al. 2015. "Cure shrinkage monitoring and process analysis of CFRP laminates with interlaminar-resin layer" *Journal of the Japan Society for Composite Materials*, 41(5): 168-175